Hindawi Publishing Corporation
Active and Passive Electronic Components
Volume 2011, Article ID 713129, 4 pages
doi:10.1155/2011/713129

Research Article

Characterization of Series Resistance and Mobility Degradation Parameter and Optimizing Choice of Oxide Thickness in Thin Oxide *N*-Channel MOSFET

Noureddine Maouhoub and Khalid Rais

Laboratoire d'Électronique, d'Instrumentation et de Traitement du Signal, Equipe de Caractérisation des Composants à Semi-Conducteurs, Faculté des Sciences, Université Chouaib Doukkali, BP 20, EL Jadida, Morocco

Correspondence should be addressed to Khalid Rais, rais_khalid@hotmail.com

Received 28 June 2011; Revised 10 August 2011; Accepted 10 August 2011

Academic Editor: G. Ghibaudo

We present two methods to extract the series resistance and the mobility degradation parameter in short-channel MOSFETs. The principle of the first method is based on the comparison between the exponential model and the classical model of effective mobility and for the second method is based on directly calculating the two parameters by solving a system of two equations obtained by using two different points in strong inversion at small drain bias from the characteristic I_d (V_g). The results obtained by these techniques have shown a better agreement with data measurements and allowed in the same time to determine the surface roughness amplitude and its influence on the maximum drain current and give the optimal oxide thickness.

1. Introduction

Accurate model parameter extraction is crucial for modeling modern MOSFET devices. Extensive work abounds in the literature dedicated to this subject. Free-carrier mobility degradation and source-and-drain series resistance are two parameters of special importance for MOSFET characterization that are particularly cumbersome to extract independently from each other. Both of these parameters produce similar effects on the device's transfer characteristics, I_d (V_g), a fact that complicates their accurate extraction.

Several ingenious procedures have been proposed to circumvent this difficulty [1–5]. Another method was proposed to extract these parameters from the drain current versus gate voltage characteristics in the saturation region using several devices of different mask channel lengths [6]. An alternative procedure was recently proposed to extract the source-and-drain series resistance independently of mobility degradation by using bias conditions under which the channel carrier mobility is kept constant [7]. Another recent works presented direct fitting and direct calculating methods in strong inversion and by exploiting the characteristic I_d (V_g) [8, 9].

In what follows we present a two procedures to be applied to the strong inversion I_d (V_g) characteristics of a single transistor, measured at a small drain bias. It is based on the exploiting of exponential model of effective mobility. The procedure has been validated using data from a single experimental short channel device.

The drain current, I_d, at very small drain bias, can be expressed in terms of intrinsic voltages as

$$I_d = \frac{W}{L} \cdot \mu_{\text{eff}} \cdot C_{\text{ox}} \cdot (V_G - V_t) \cdot V_D, \qquad (1)$$

where W is the channel width, L is the channel length, C_{ox} is the oxide capacitance, μ_{eff} is the effective free-carrier mobility, V_G is the intrinsic gate voltage, V_D the intrinsic drain voltage, and V_t is the threshold voltage.

If the source-and-drain series resistance is significant, the device's intrinsic gate and drain voltages are

$$V_G = V_g - I_d \cdot \frac{R_{\text{sd}}}{2}, \qquad V_D = V_d - I_d \cdot R_{\text{sd}}, \tag{2}$$

where V_g and V_d are the externally applied gate and drain voltages, respectively, and R_{sd} is the total source-and-drain series resistance.

The model of variation mobility with effective field considers that the attenuation of effective mobility is particularly due to Surface Roughness Scattering [10]. This work generalized all the classical models [9, 11] and give a physical meaning to the different used parameters.

The effective mobility is given by the exponential model in strong inversion:

$$\mu_{\text{eff}} = \mu_0 \cdot \exp(-\theta_i \cdot (V_G - V_t)), \tag{3}$$

where

$$\theta_i = \frac{\eta \cdot \beta \cdot \Delta \cdot C_{\text{ox}}}{\varepsilon_{\text{si}}}. \tag{4}$$

θ_i is the intrinsic attenuation coefficient of mobility, η is constant parameter equal to 0.5 for electrons and 0.33 for holes, $\beta = q/kT$ is the inverse of the thermal potential, ε_{si} is the silicon permittivity, Δ is the surface roughness amplitude, and μ_0 represents the low-field mobility.

Assuming that $V_g - V_t \gg I_d \cdot R_{\text{sd}}/2$, relation (1) becomes

$$I_d = K \cdot \frac{(V_g - V_t)}{\exp(\theta_i \cdot (V_g - V_t)) + ((K \cdot R_{\text{sd}})/V_d) \cdot (V_g - V_t)}, \tag{5}$$

where

$$K = \frac{W}{L} \cdot \mu_0 \cdot C_{\text{ox}} \cdot V_d. \tag{6}$$

Introducing the series resistance effect, the effective mobility becomes

$$\mu_{\text{eff}} = \frac{1}{(1/(\mu_0 \cdot \exp[-\theta_i \cdot (V_g - V_t)])) + \theta_{R\,\text{sd}}(V_g - V_t)}, \tag{7}$$

where

$$\theta_{R\,\text{sd}} = \frac{K \cdot R_{\text{sd}}}{V_d}. \tag{8}$$

The transconductance is given by

$$g_m = \frac{dI_d}{dV_g} = K \cdot \frac{(1 - \theta_i \cdot (V_g - V_t)) \exp(\theta_i \cdot (V_g - V_t))}{[\exp(\theta_i \cdot (V_g - V_t)) + \theta_{R\,\text{sd}} \cdot (V_g - V_t)]^2}. \tag{9}$$

2. First Method

According to the classical model [10], and for low fields, the comparison of the first-order development of the exponential term in relation (3) gives the relation between the intrinsic coefficient attenuation mobility in exponential model and its value extrinsic θ_e in the classical model:

$$\theta_e = \theta_i + \theta_{R\,\text{sd}}. \tag{10}$$

The values of K and θ_e are determined, respectively, by the slope in the plot of $Y_0(V_g) = I_d/\sqrt{g_m}$ and $H_0(V_g) = 1/\sqrt{g_m}$ which are straight line at relative low field.

For thin oxide and at high field, the characteristic $Y(V_g) = I_d/\sqrt{g_m}$, which has the advantage to be independent of series resistance, presents a deviation with regard to $Y_0(V_g)$.

We note that g_m can reach the value zero at V_{gm}:

$$\theta_i = \frac{1}{(V_{gm} - V_t)}. \tag{11}$$

Experimentally we use the device below this value, meanwhile we use the characteristic $(Y(V_g)/Y_0(V_g) - 1)$ versus V_g. The value at ten per; cent of this characteristic is corresponding to the critical value $(V_{gm} - V_t)/2 = 1/2\theta_i$; combining (11) with relations (3) and (10) we obtain the surface roughness amplitude Δ and series resistance R_{sd}, respectively.

3. Second Method

The procedure involves first extracting the expression $\exp(\theta_i(V_g - V_t))$ from the drain current equation and using the function $Y = I_d/\sqrt{g_m}$.

Setting $x = V_g - V_t$, and after some mathematical manipulation we obtain the following expression:

$$\frac{Y^{-2} \cdot x}{1 - \theta_i \cdot x} = \frac{1}{I_d} - \frac{R_{\text{sd}}}{V_d}. \tag{12}$$

Secondly, we choose two points in the characteristic I_d (V_g) in strong inversion V_{g1} and V_{g2} (x_1 and x_2), and we solve the following system:

$$\begin{aligned} \frac{Y^{-2}(V_{g1}) \cdot x_1}{1 - \theta_i \cdot x_1} &= \frac{1}{I_d(V_{g1})} - \frac{R_{\text{sd}}}{V_d}, \\ \frac{Y^{-2}(V_{g2}) \cdot x_2}{1 - \theta_i \cdot x_2} &= \frac{1}{I_d(V_{g2})} - \frac{R_{\text{sd}}}{V_d}. \end{aligned} \tag{13}$$

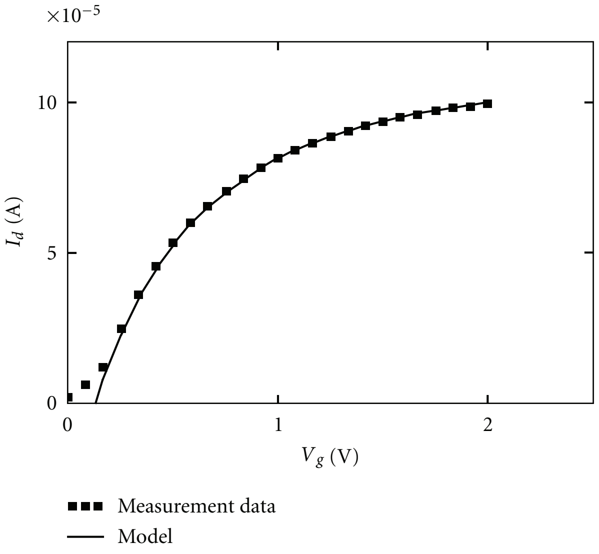

Figure 1: Transfer characteristics (symbols). Also shown is the corresponding model (continuous line) obtained from the drain current model using the calculated parameters (Table 1).

Determining the parameter θ is done using the subtraction of the two system equations; we obtain a second order equation whose appropriate solution is:

$$\theta_i = \frac{(B \cdot x_1 + C \cdot x_2 + C \cdot x_1 - A \cdot x_2)}{2 \cdot C \cdot x_1 \cdot x_2} + \frac{\sqrt{(B \cdot x_1 + C \cdot x_2 + C \cdot x_1 - A \cdot x_2)^2 + 4 \cdot x_1 \cdot x_2 \cdot (A - B - C)}}{2 \cdot C \cdot x_1 \cdot x_2}, \tag{14}$$

where

$$\begin{aligned} A &= Y^{-2}\left(V_{g1}\right) \cdot x_1, \\ B &= Y^{-2}\left(V_{g2}\right) \cdot x_2, \\ C &= \frac{1}{I_d\left(V_{g1}\right)} - \frac{1}{I_d\left(V_{g2}\right)}. \end{aligned} \tag{15}$$

The series resistance expression can be written using one of the two system equations:

$$R_{\mathrm{sd}} = V_d \cdot \left(\frac{1}{I_d\left(V_{g2}\right)} - \frac{Y^{-2}\left(V_{g2}\right) \cdot x_2}{1 - \theta_i \cdot x_2} \right). \tag{16}$$

The choice of V_{g1} and V_{g2} is determined in mobility degradation effect zone.

4. Results and Discussion

In order to validate the previous procedures, the device used in this work has the parameters: channel width $W = 4\,\mu$m, gate oxide thickness $t_{\mathrm{ox}} = 5$ nm, channel length $L = 0.1\,\mu$m, and channel doping Na $= 10^{16}$ cm^{-3}.

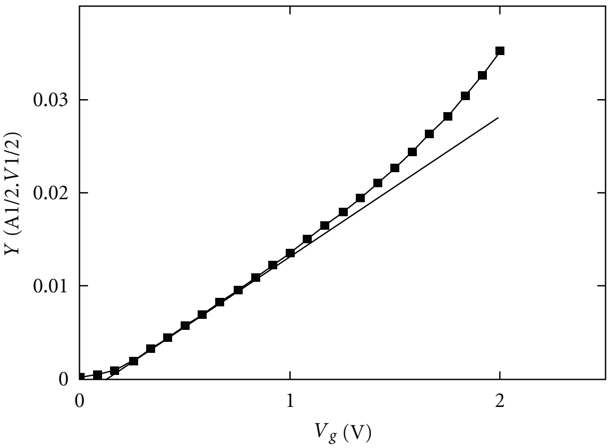

Figure 2: Characteristic Y versus gate voltage.

Table 1: Values of the different extracted parameters.

Parameter	θ_i (1/V)	R_{sd} (Ω)	Δ (nm)
First method	0.363	107.53	0.31
Second method	0.36	108.8	0.28

The transfer characteristics were measured at a small drain voltage: $V_d = 20$ mV. The application of our model with calculated parameters (Table 1) shows a good agreement with experimental data (Figure 1).

In relatively weak field we use model (1) as an approximation of our model; we plot this function $Y(V_g)$. The parameter V_t can be extracted from the V_g axis intercept of the observed straight lines of Y versus V_g plot (Figure 2).

Figure 3 shows the characteristic $(Y(V_g)/Y_0(V_g) - 1)$ versus V_g which allows determining the intrinsic attenuation parameter.

5. Optimization of Drain Current

At $V_g = V_{gm}$, the drain current is maximal, its value is

$$I_{d\max} = \frac{V_d}{R_{\mathrm{ch\ min}} + R_{\mathrm{sd}}}, \tag{17}$$

where $R_{\mathrm{ch\ min}}$ is the minimal resistance of channel:

$$R_{\mathrm{ch\ min}} = \frac{\Delta\beta\eta L}{W\mu_0\varepsilon_{\mathrm{si}}} \cdot e. \tag{18}$$

We note its independence of the oxide thickness and its proportionality of the surface roughness amplitude and of the channel length.

On the other hand, if we plot I_d versus the oxide thickness t_{ox} for a given gate voltage V_g (Figure 4), we can find the optimal oxide thickness. In fact, for very thin oxide the collisions on surface roughness predominate, and for thick oxide the inversion charge decreases, and consequently the drain current.

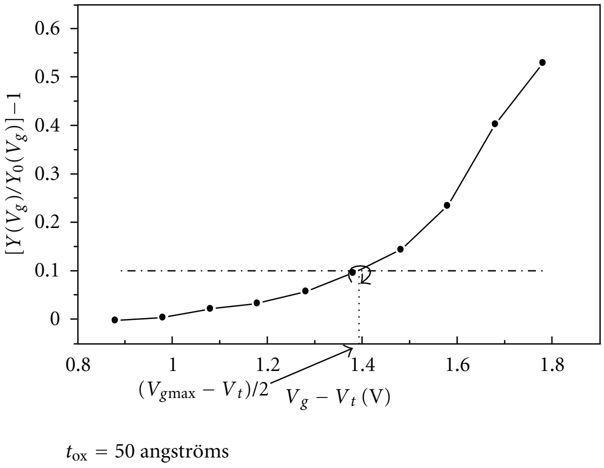

FIGURE 3: Characteristic $Y(V_g)$ to $Y_0(V_g)$ ratio versus gate voltage.

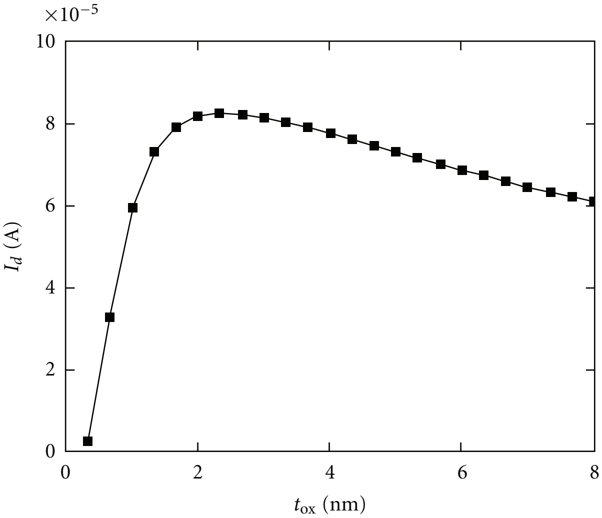

FIGURE 4: Drain current versus oxide thickness for $V_g = 1.5$ V.

6. Conclusion

We have presented two procedures that permit us to extract the mobility degradation factor, the series resistance, and the surface roughness thickness of MOSFET using the exponential model of mobility. The procedures are simple and accurate and based on calculating the model parameters using the experimental data measured in strong inversion at small drain bias. The exponential model of mobility allows also us to optimize the oxide thickness for the transistor.

References

[1] C. L. Lou, W. K. Chim, D. S. H. Chan, and Y. Pan, "A novel single-device DC method for extraction of the effective mobility and source-drain resistances of fresh and hot-carrier degraded drain-engineered MOSFET's," *IEEE Transactions on Electron Devices*, vol. 45, no. 6, pp. 1317–1323, 1998.

[2] G. M. Lim, Y. C. Kim, D. J. Kim, Y. W. Park, and D. M. Kim, "Additional resistance method for extraction of separated nonlinear parasitic resistances and effective mobility in MOSFET's," *Electronics Letters*, vol. 36, no. 14, pp. 1233–1234, 2000.

[3] C. S. Ho, Y. C. Lo, Y. H. Chang, and J. J. Liou, "Determination of gate-bias dependent source/drain series resistance and effective channel length for advanced MOS devices," *Solid-State Electronics*, vol. 50, no. 11-12, pp. 1774–1779, 2006.

[4] P. R. Karlsson and K. O. Jeppson, "An efficient method for determining threshold voltage, series resistance and effective geometry of MOS transistors," *IEEE Transactions on Semiconductor Manufacturing*, vol. 9, no. 2, pp. 215–222, 1996.

[5] C.-Y. Lu and J. A. Cooper Jr., "A new constant-current technique for MOSFET parameter extraction," *Solid-State Electronics*, vol. 49, no. 3, pp. 351–356, 2005.

[6] F. J. García-Sánchez, A. Ortiz-Conde, A. Cerdeira, M. Estrada, D. Flandre, and J. J. Liou, "A method to extract mobility degradation and total series resistance of fully-depleted SOI MOSFET's," *IEEE Transactions on Electron Devices*, vol. 49, no. 1, pp. 82–88, 2002.

[7] D.-W. Lin, M.-L. Cheng, S.-W. Wang, C.-C. Wu, and M.-J. Chen, "A constant-mobility method to enable MOSFET series-resistance extraction," *IEEE Electron Device Letters*, vol. 28, no. 12, pp. 1132–1134, 2007.

[8] A. Ortiz-Conde, F. J. García-Sánchez, J. Muci et al., "Indirect fitting procedure to separate the effects of mobility degradation and source-and-drain resistance in MOSFET parameter extraction," *Microelectronics Reliability*, vol. 49, no. 7, pp. 689–692, 2009.

[9] J. Muci, D. C. L. Muñoz, Á. D. L. Rey et al., "A new integration-based procedure to separately extract series resistance and mobility degradation in MOSFET's," *Semiconductor Science and Technology*, vol. 24, no. 10, 105015, 6 pages, 2009.

[10] A. El Abbassi, Y. Amhouche, E. Bendada, R. Rmaily, and K. Raïs, "Characterization of series resistances and mobility attenuation phenomena in short channel MOS transistors," *Active and Passive Electronic Components*, vol. 24, no. 1, pp. 13–22, 2001.

[11] G. Ghibaudo and F. Balestra, "Modelling of ohmic MOSFET operation at very low temperature," *Solid State Electronics*, vol. 31, no. 1, pp. 105–108, 1988.


Journal of
Engineering


The Scientific World Journal


International Journal of
Rotating Machinery


Journal of
Sensors


International Journal of
Distributed Sensor Networks

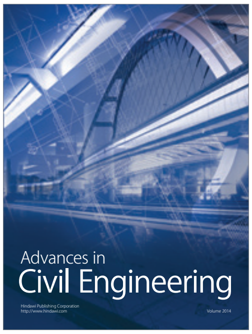
Advances in
Civil Engineering

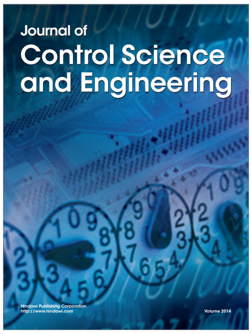
Journal of
Control Science and Engineering


Journal of
Robotics


Journal of
Electrical and Computer Engineering

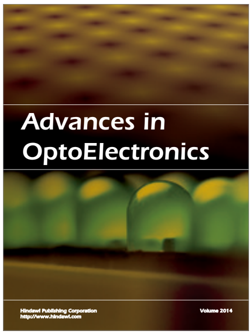
Advances in
OptoElectronics


VLSI Design


International Journal of
Navigation and Observation

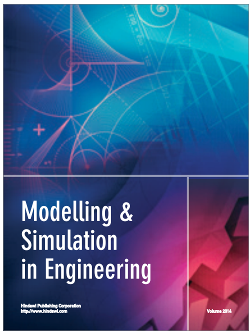
Modelling &
Simulation
in Engineering


International Journal of
Aerospace Engineering

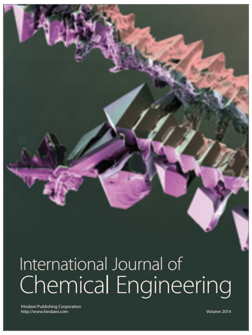
International Journal of
Chemical Engineering

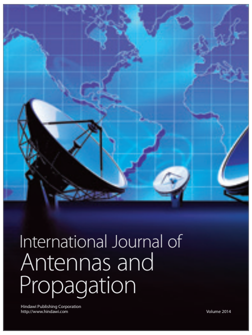
International Journal of
Antennas and Propagation


Active and Passive
Electronic Components

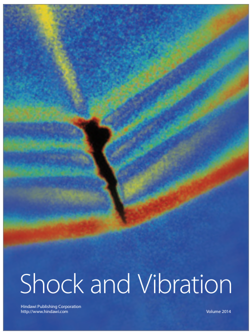
Shock and Vibration

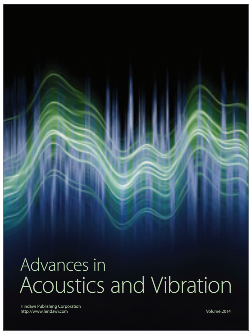
Advances in
Acoustics and Vibration